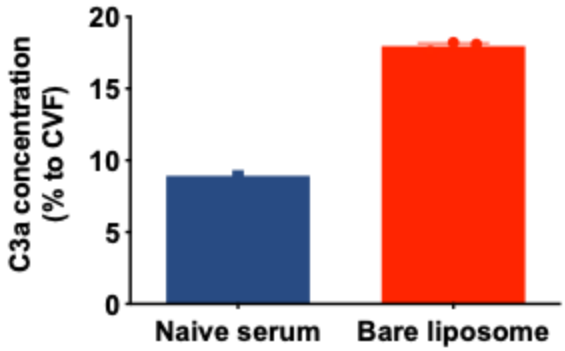

Supplementary Figure 1. Complement activation by bare PEGylated-liposomes. Bare liposomes induced a 2.0-fold increase in C3a, relative to naive serum levels.

A

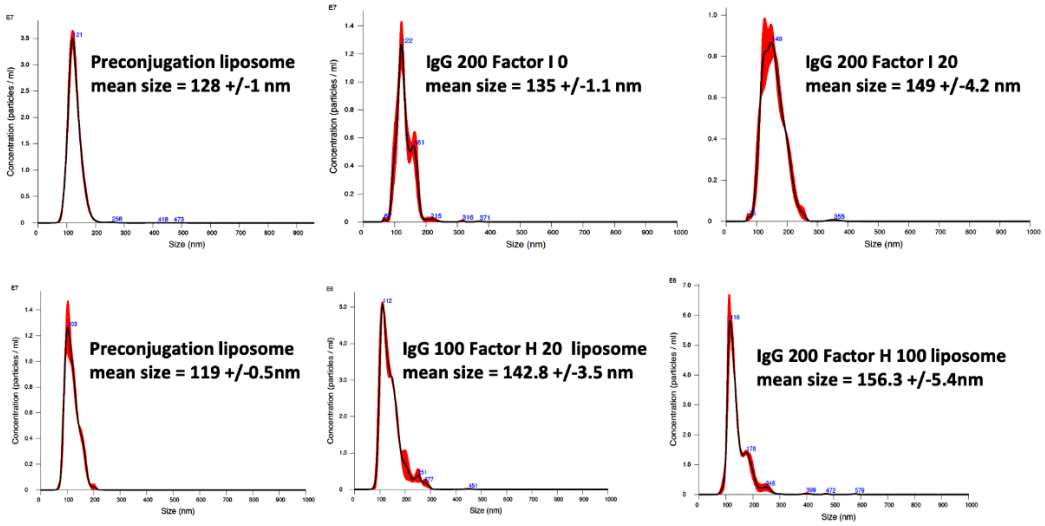

B

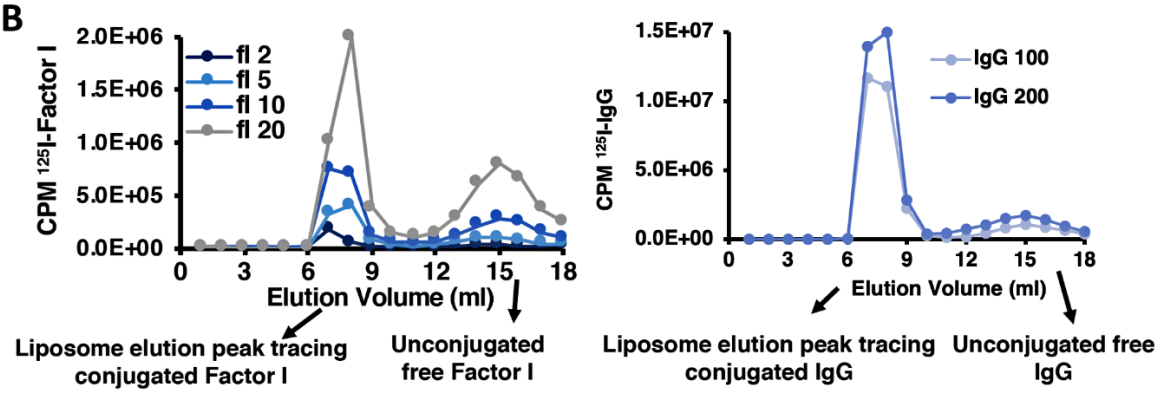

C

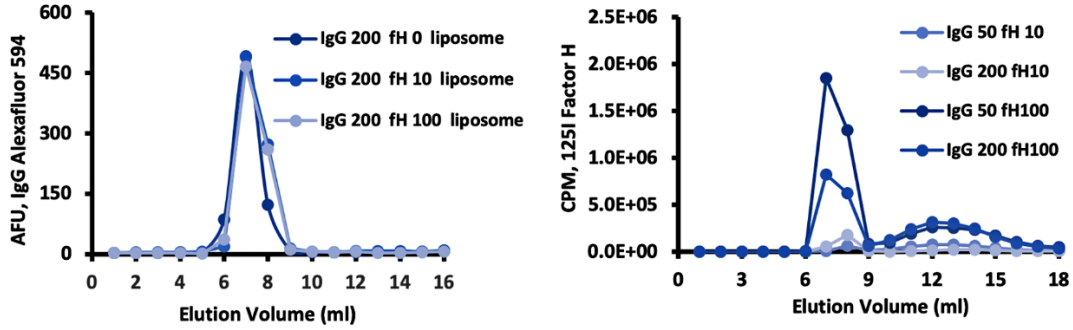

D

Liposome size	Size (nm)	PDI
Unconjugated liposomes (n=16)	136 +/- 8.9	0.09
IgG liposomes (n=8)	157.2 +/- 5.0	0.10
IgG + Factor I (n=12)	160.8 +/- 8.0	0.12
IgG + Factor H (n=8)	162.7 +/- 13	0.18

Supplementary Figure 2. Characterization of complement protein liposomes. (a) Nanoparticle tracking analysis determination of size distributions (per size concentration represented as number of particles per mL) for liposomes with either Factor I (top panels) or Factor H (bottom panels) conjugated alongside IgG. Plots show triplicate measurement overlays for each formulation type. Leftmost panels show liposome size distributions before conjugation to proteins. Middle top panel: Liposomes with IgG and no Factor I. Right top panel: Liposomes with IgG and 20 Factor I. Middle bottom panel: Liposomes with 100 IgG and 20 Factor H. Right bottom panel: Liposomes with 200 IgG and 100 Factor H. (b-c) Sepharose column chromatography traces indicating efficiency of protein-liposome conjugation reactions. (b), left panel: Chromatography tracing ^{125}I-Factor I binding to liposomes with IgG (IgG not traced in this data). Factor I that is not conjugated to liposomes elutes broadly from 11-18 mL. Factor I that is conjugated to liposomes elutes from 6-9 mL. Conjugation efficiency was calculated by the ratio of area under the curve of the liposome peak to the sum of the liposome peak and the free Factor I peak. Efficiency of Factor I conjugation: 30-77%, variable with respect to the number of Factor I in the conjugation reaction. (b), right panel: Chromatography tracing ^{125}I-IgG conjugation to liposomes with Factor I (Factor I not traced in this data), as in the left panel for ^{125}I-Factor I. IgG conjugation efficiency was >85% for both 100 and 200 IgG per liposome. (c), right panel: Chromatography tracing ^{125}I-Factor H binding to liposomes at 2 coating densities of both IgG and Factor H. Factor H that is not conjugated to liposomes elutes broadly from 11-18 mL. Factor H that is conjugated to liposomes elutes from 6-9 mL. Conjugation efficiency was calculated by the ratio of area under the curve of the liposome peak to the sum of the liposome peak and the free Factor H peak. Efficiency of Factor H conjugation varied from 57-78%. (c), left panel: Chromatography tracing fluorescent IgG-DBCO binding to liposomes with varying amounts of Factor H and IgG. IgG not bound to liposomes elutes at ~14 ml and IgG bound to liposomes elutes from 6-9 mL. IgG-liposome conjugation efficiency, calculated as above for Factor I and Factor H, was >95% for all quantities of Factor H and IgG. (d) Tabulated size and PDI data for unconjugated, IgG-conjugated, and IgG+Factor I- or IgG+Factor H-conjugated liposomes. Tabulated data in (d) represents average liposome size derived from analysis as in (a) over multiple preparations, with number of preparations noted in the table.

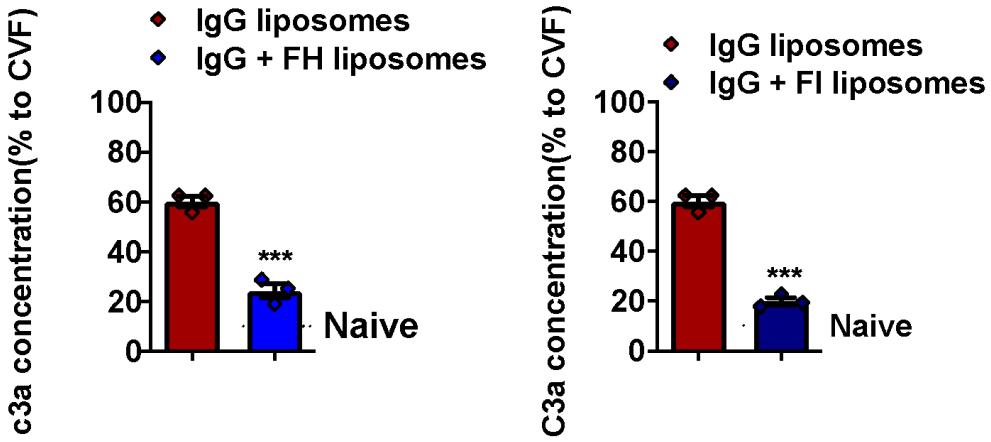

Supplementary Figure 3. Comparison of C3a generation by IgG liposomes vs. C3a generation by IgG liposomes with factor H included at 20 per liposome (left panel) or with factor I included at 20 per liposome (right panel).

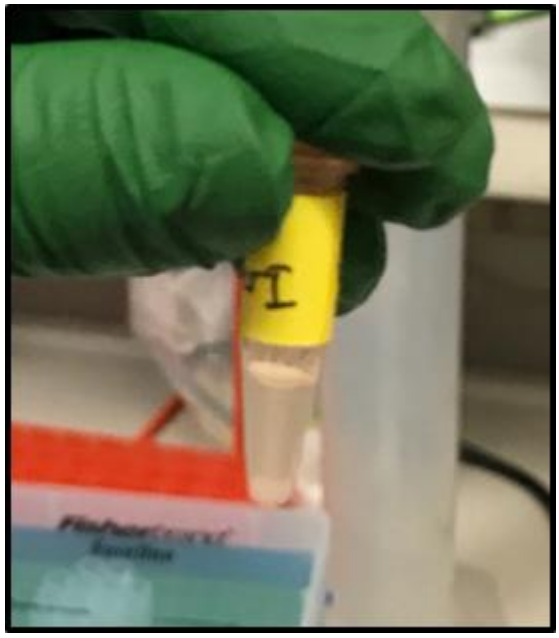

Supplementary Figure 4. Factor H liposomes flocculated after conjugation.

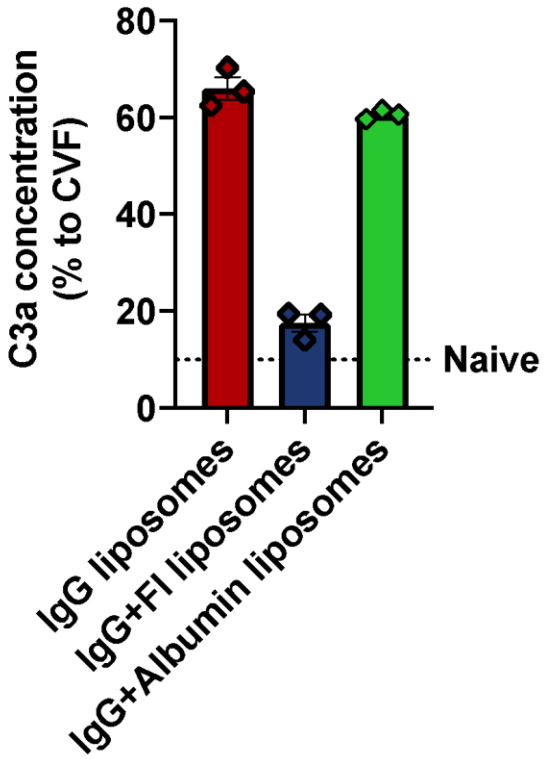

Supplementary Figure 5. Comparison of factor I effects on C3a generation by IgG liposomes vs. irrelevant protein (albumin) effects on C3a generation by IgG liposomes. Data is identical to the inset in figure 1, panel D, but indicates the C3a level in naive serum by dashed line.

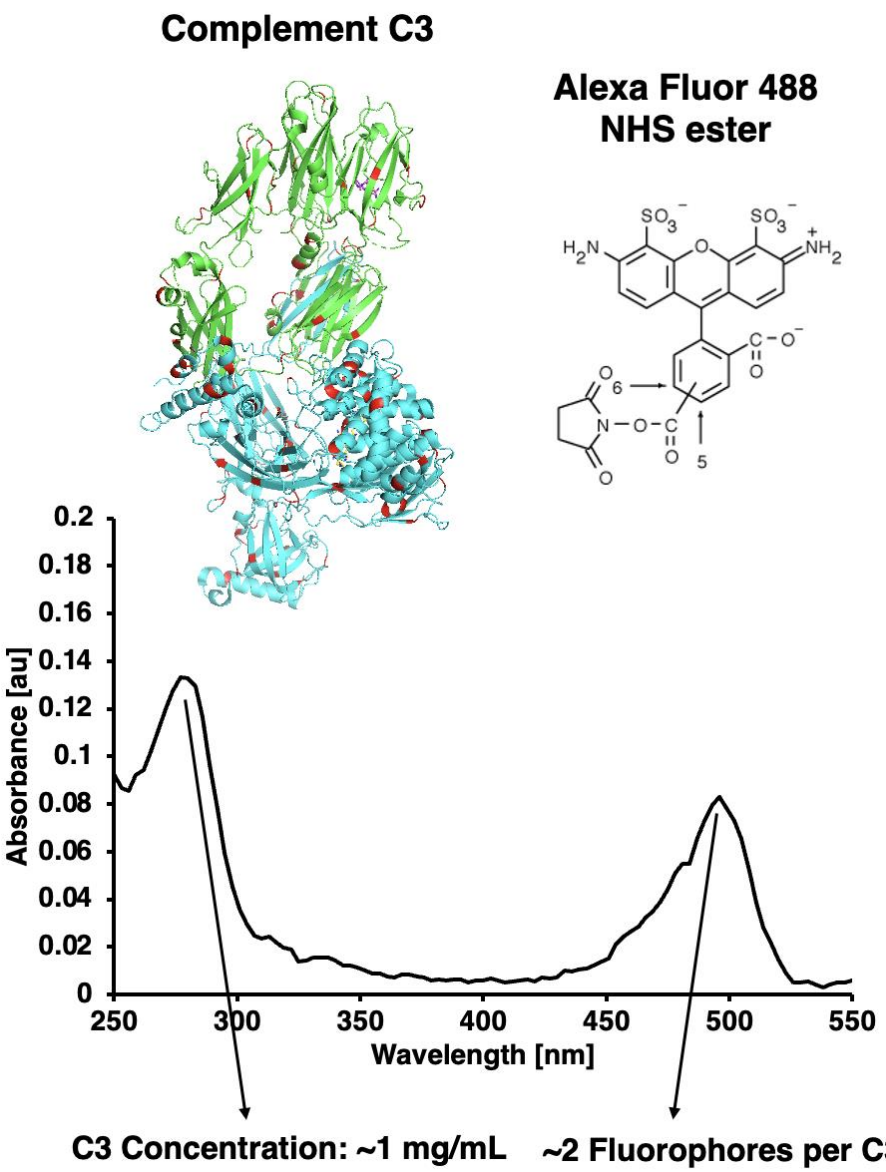

Supplementary Figure 6. Upper panels: cartoon of human complement protein C3 represents lysines, to which Alexa Fluor 488 NHS ester can conjugate, in red. Lower panel: Spectrophotometric verification of complement protein C3 labeling with Alexa Fluor 488 NHS ester.

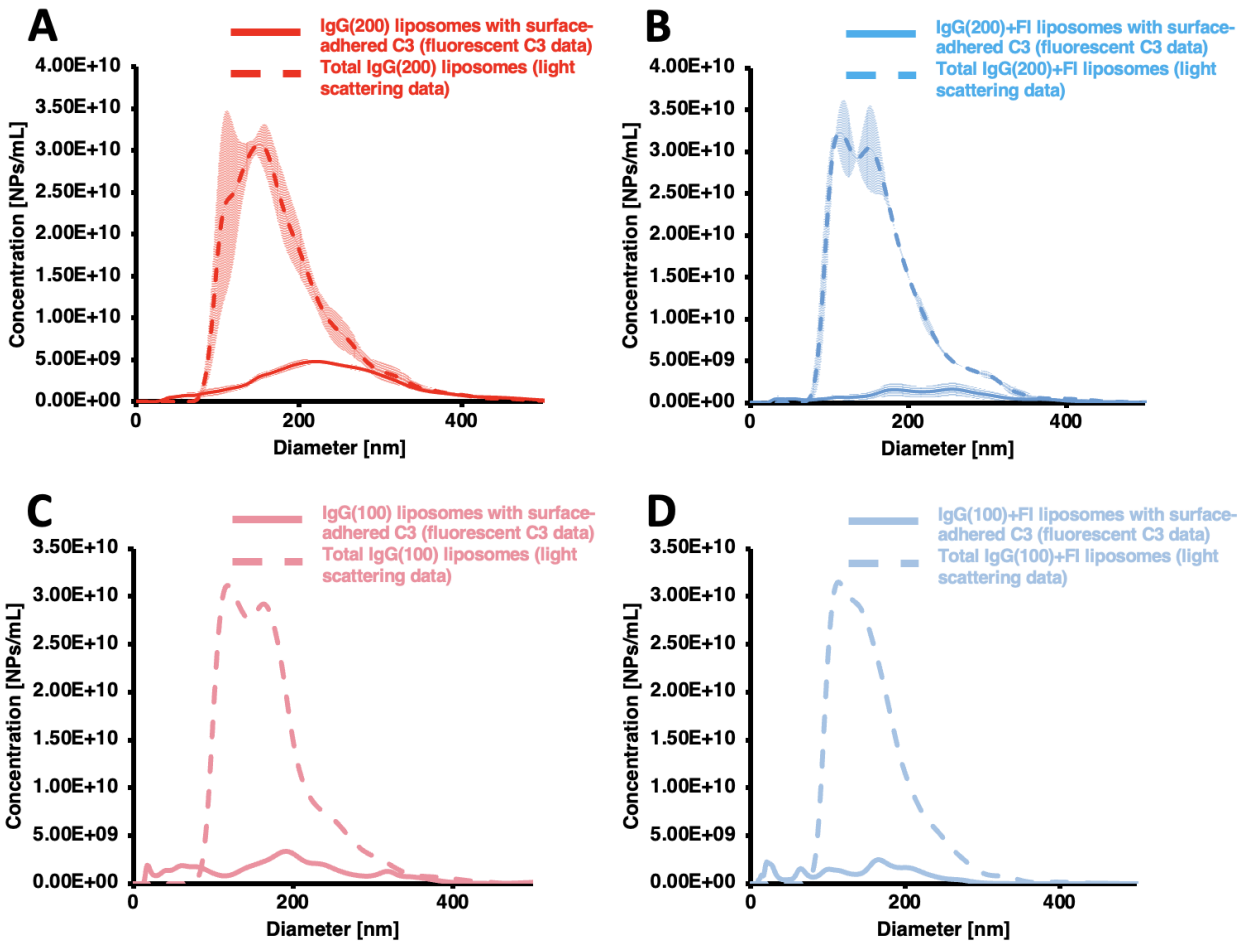

Supplementary Figure 7. Nanoparticle tracking analysis results comparing liposome sizing and counting via light scattering in buffer (dashed lines) vs. liposome sizing and counting via surface-adsorbed C3 fluorescence (solid lines) for: (a) IgG liposomes with high IgG surface density; (b) IgG+Factor I liposomes with high IgG surface density; (c) IgG liposomes with low IgG surface density; (d) IgG+Factor I liposomes with low IgG surface density.

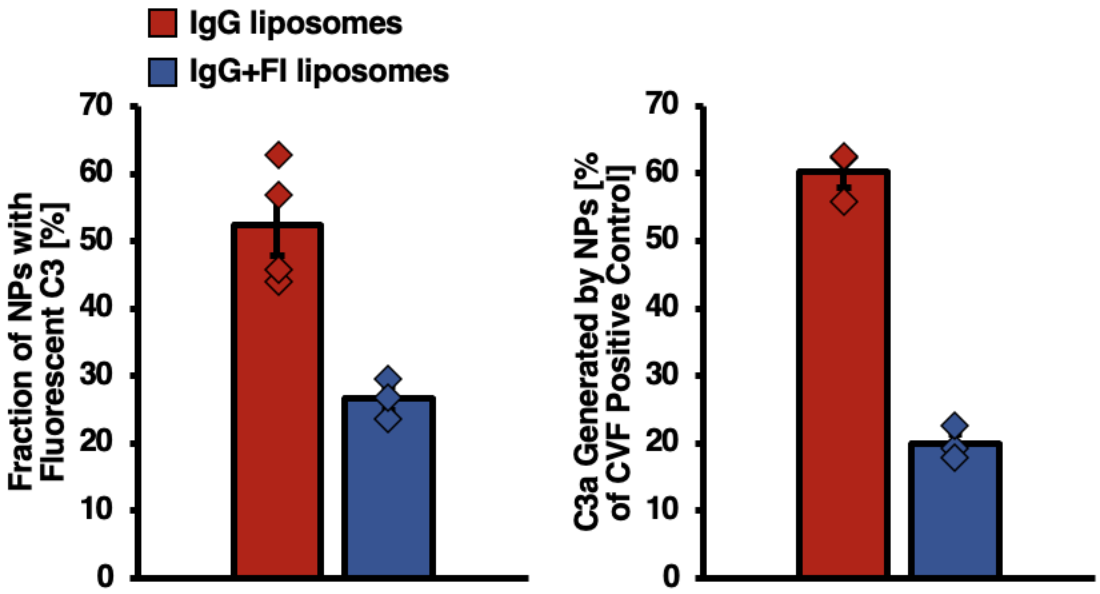

Supplementary Figure 8. Complement activation by IgG liposomes, with or without factor I on the liposome surfaces. The figure compares measurement of factor I effects by fluorescent C3 detection in nanoparticle tracking analysis assays with measurement of factor I effects by C3a ELISA, showing similar effects with each metric.

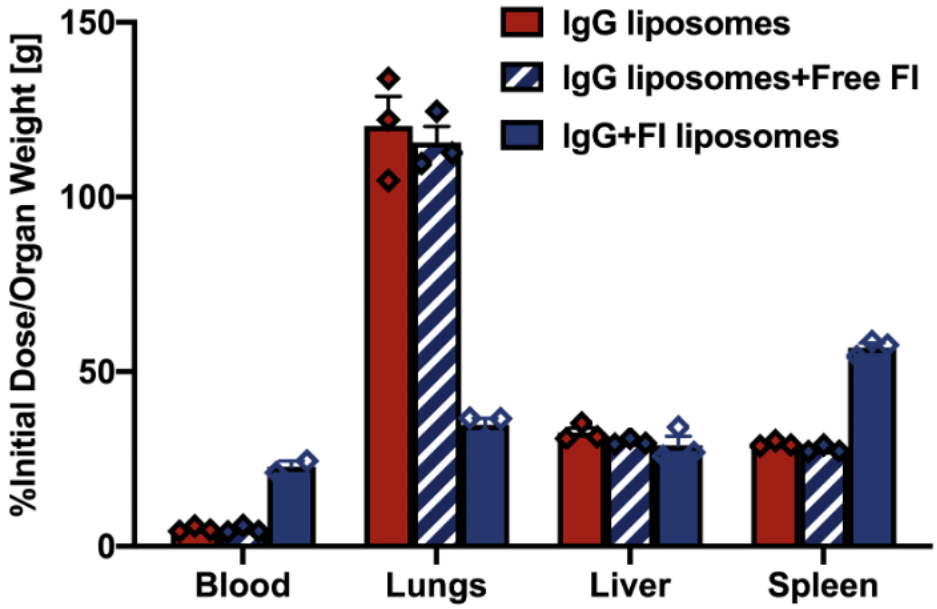

Supplementary Figure 9. Biodistributions of IgG liposomes in mice subject to intravenous LPS injury. The data compares IgG liposomes alone vs. IgG liposomes co-injected with factor I vs. IgG liposomes conjugated to an equivalent quantity of factor I to that provided in the co-injected dose. The data indicate that factor I extended IgG liposome circulation time and reduced non-specific lung uptake only when conjugated to the IgG liposome surface.

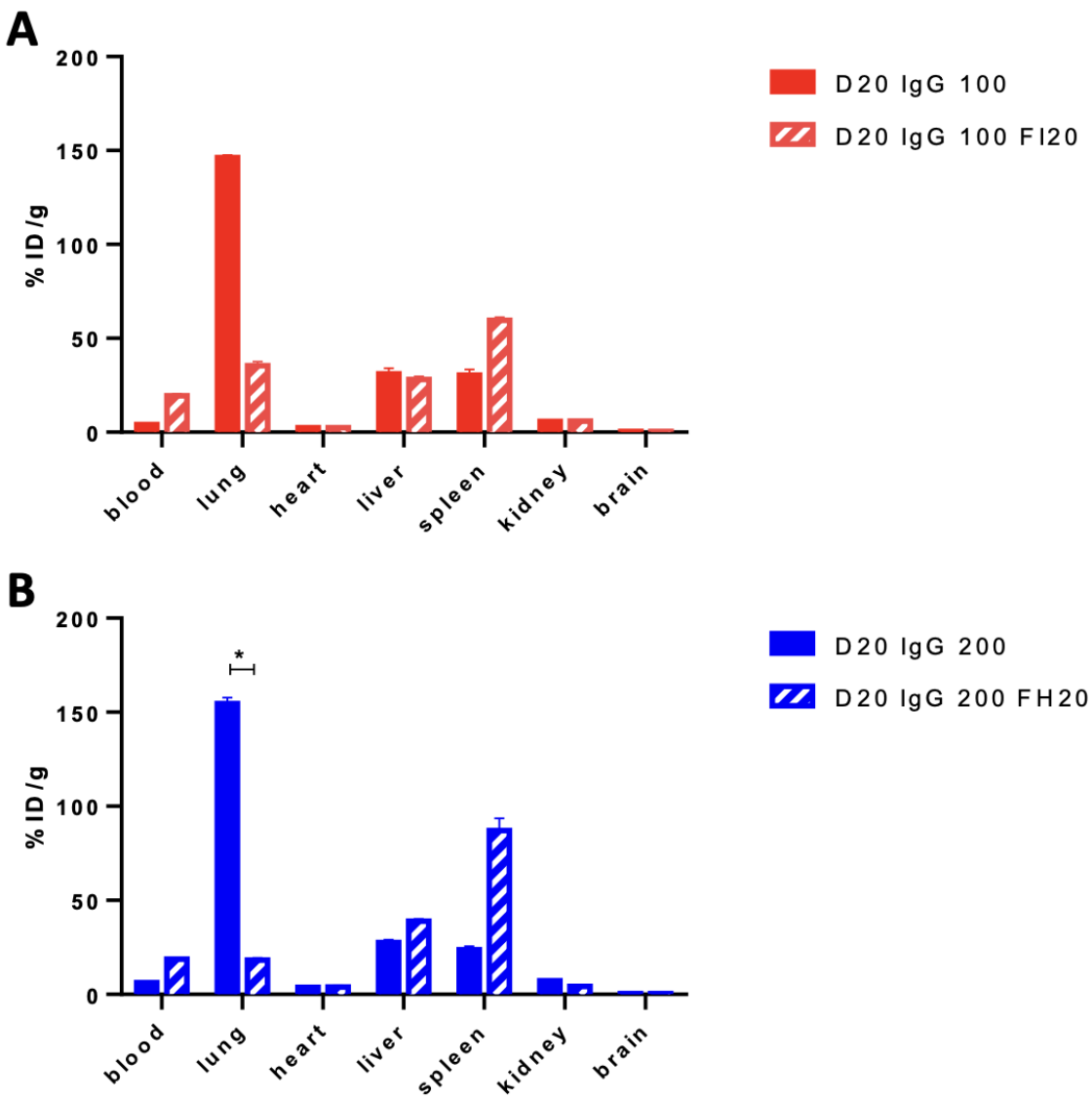

Supplementary Figure 10. (a) Full data for biodistributions of IgG and IgG+Factor I liposomes in IV-LPS-affected mice, as represented partially in main text figure 2a. (b) Analogous data for comparison of IgG and IgG+Factor H liposomes in IV-LPS-affected mice.

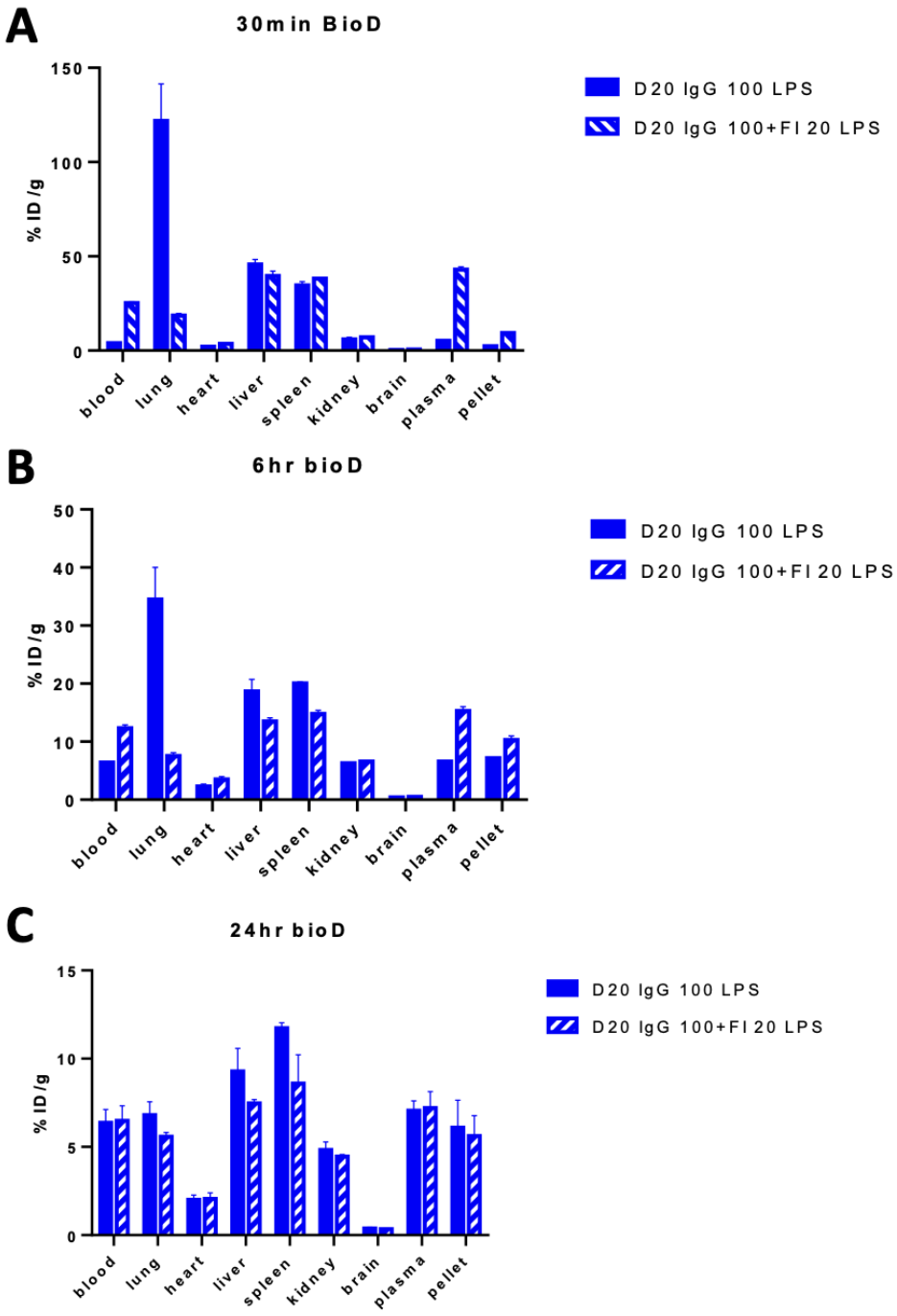

Supplementary Figure 11. (a-c) Full data for biodistributions of IgG and IgG+Factor I liposomes at different time points after liposome injection, as represented partially in main text figure 2b.

	IgG liposomes (Naive)			IgG+FI liposomes (Naive)			IgG liposomes (LPS)			IgG+FI liposomes (LPS)		
Hours	**Mean**	**SEM**	**N**	**Mean**	**SEM**	**N**	**Mean**	**SEM**	**N**	**Mean**	**SEM**	**N**
0.08333	22.64	2.39	3	23.3	2.81	3	11.3	1.34	3	37.67	1.82	3
0.25	8.96	0.23	3	10.76	1.62	3	4.56	0.45	3	28.27	1.29	3
0.5	6.15	0.34	3	7.61	0.67	3	3.98	0.22	3	25.22	0.65	3
2	5.23	0.6	3	8.05	0.69	3	5.69	0.03	3	19.81	0.64	3
4	4.75	0.72	3	6.6	0.32	3	6.41	0.18	3	15.68	0.66	3
6	3.47	0.45	3	5.27	0.34	3	6.41	0.08	3	12.31	0.6	3
24	0.66	0.01	3	1.04	0.11	3	6.37	0.75	3	6.48	0.84	3

Supplementary Figure 12. Raw data table of Figure 2C, blood pharmacokinetics of IgG liposomes or IgG+FI liposomes in naive or IV-LPS challenged mice. Note that in mice that received LPS (a model of sepsis), the time series plot of nanoparticle concentration in the blood shows a dip and then increase (Figure 2d), which is quite different than the classic bi-exponential decay typical of most drugs' concentration in blood. As we showed in Myerson et al, 2021 [19], in IV-LPS mice, complement-opsonized nanoparticles also display a rapid dip in blood concentration, followed by a slower rebound (increase) in blood concentration. In that paper, we showed that the initial dip in such nanoparticles' blood concentration is due to the rapid uptake of the nanoparticles by neutrophils that are marginated in the lungs (i.e., these cells reside in the lungs' capillary lumens). After that initial dip, we showed that the rebound (increase) in blood concentration is due to a slow demargination of neutrophils (leaving the marginated state to circulate in blood), and that those demarginated neutrophils contain the nanoparticles or catabolized fragments thereof. Among our several lines of proof for this mechanism, we showed: 1) increased neutrophil numbers in the blood after nanoparticle delivery, and a decreased number of neutrophils in the lungs; 2) within the blood of these mice, we noted an increase in the relative fraction of nanoparticles (radiotraced) in the cell pellet (where circulating neutrophils reside) vs. plasma.

Parameter	**IgG 100 (Naïve)**	**IgG 100/FI 20 (Naïve)**	**IgG 100 (LPS)**	**IgG 100/FI 20 (LPS)**
$AUC^{0\text{-}24\ h}$ (%ID/g*h)	68.2±11.5	101±10	150±7	279±2
AUC^{inf} (%ID/g*h)	75.6±10.6	113±11	N.D.	493±65
% AUC Extrapolated	9.95±2.77	10.3±2.5	N.D.	41.1±9.1
$t^{1/2}$ (h)	7.70±1.11	7.70±0.85	N.D.	21.7±4.8
CL (mL/h)	1.34±0.20	0.891±0.083	N.D.	0.211±0.032
V^{ss} (mL)	12.2±3.4	8.16±1.23	N.D.	5.66±0.74

Supplementary Figure 13. Tabulated non-compartmental analysis parameters for IgG or IgG+FI liposome pharmacokinetics data in mice. Note that estimation of terminal slope was not valid for IgG liposomes in mice affected by intravenous LPS, due to the time traces not being monotonic, as described in Supplementary Figure 12. Non-compartmental analysis assumes monotonicity, and usually biexponential decay of plasma concentrations of nanoparticles. Therefore, parameters relying on the terminal slope estimate were not tabulated for these nanoparticles.

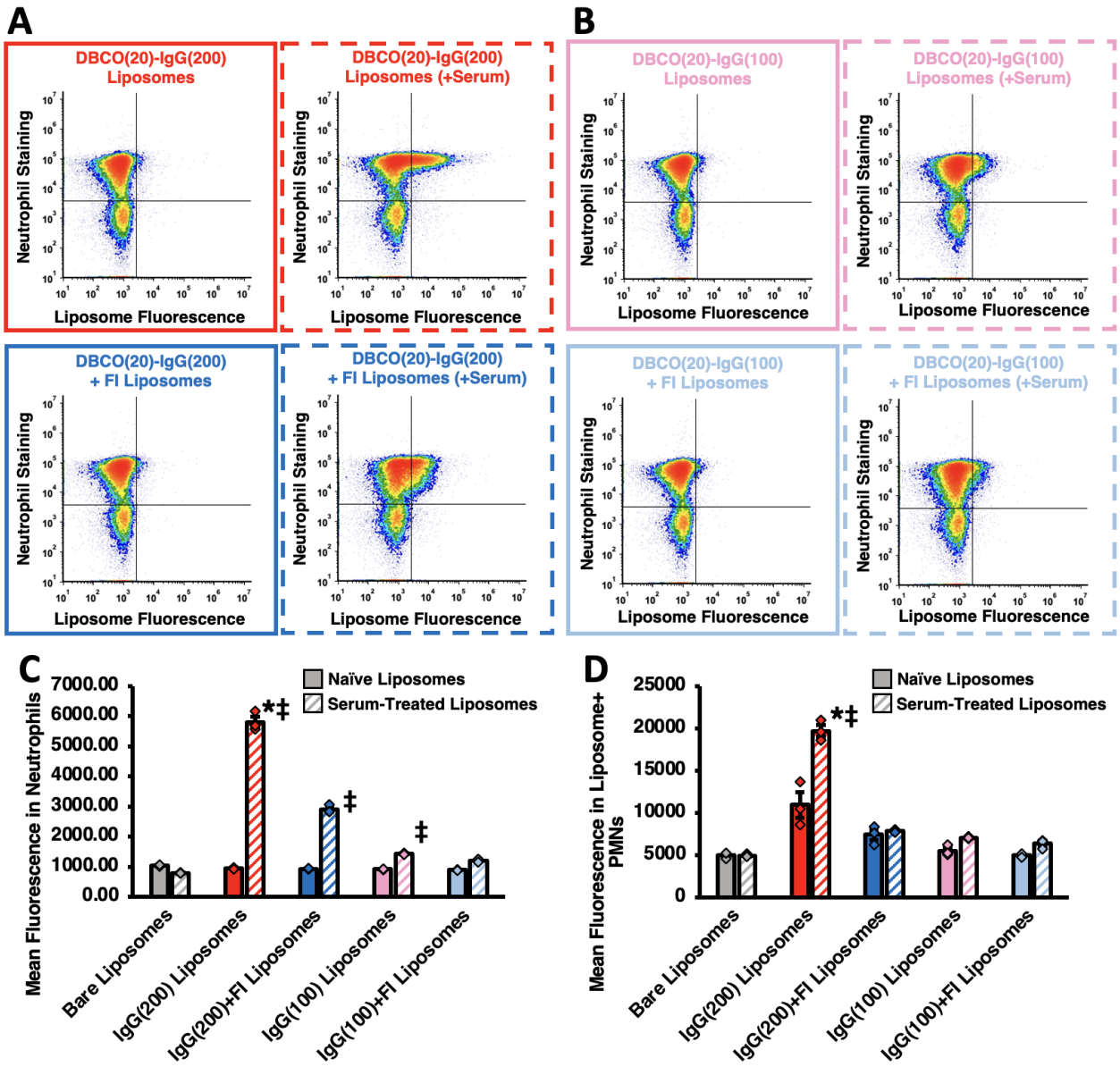

Supplementary Figure 14. (a) Flow cytometry data depicting anti-Ly6G neutrophil stain vs. liposome fluorescence following *in vitro* incubation of bone marrow-derived neutrophil-enriched cell suspensions with IgG (upper panels, red) or IgG+Factor I (lower panels, blue) liposomes. Rightmost panels (dashed outlines) indicate data for liposomes treated/opsonized in serum prior to incubation with cells. (b) Data analogous to that in (a) but for liposomes with lower IgG surface density. (c) Mean liposome fluorescence in Ly6G-positive cells for the conditions outlined in (a-b), with data for bare liposomes included for comparison. (d) Data as in (c) but gated on liposome-positive neutrophils. *: $p<1x10-10$ for comparison of serum-treated conditions for IgG liposomes with and without Factor I. ‡: $p<0.0001$ for comparison of naive and serum-treated conditions for the same liposomes.

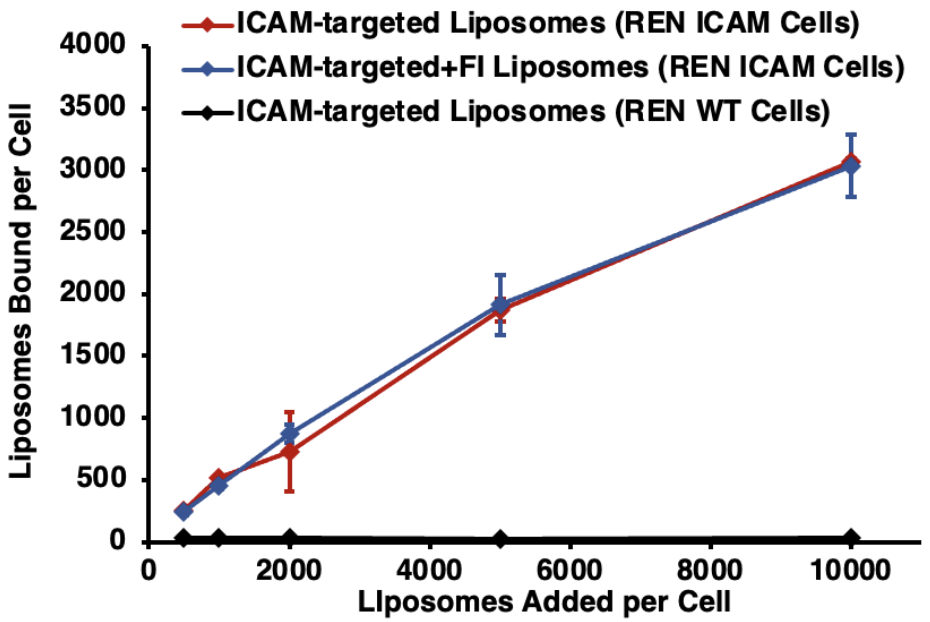

Supplementary Figure 15. Adhesion of ICAM-targeted liposomes (100 anti-ICAM mAb per liposome), with or without factor I included on the liposome surface, to ICAM-expressing REN cells. Data indicate dose-dependent adhesion of ICAM-targeted liposomes to ICAM-expressing cells, with factor I causing no change to ICAM targeting. Data for incubation of ICAM-targeted liposomes with wild-type REN cells (with no surface ICAM) is included as a negative control.

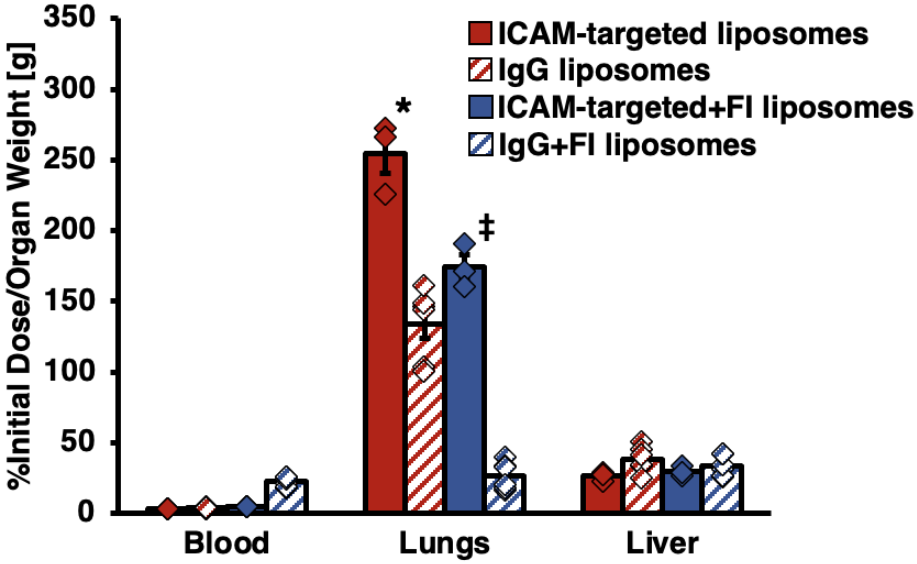

Supplementary Figure 16. Comparison of biodistribution data for ICAM-targeted vs. IgG liposomes, with or without factor I conjugated to the liposome surfaces. Data are reproduced from that depicted in figures 2 and 3 in the main text, but arranged to indicate specific lung targeting for ICAM-targeted vs. IgG liposomes. *: $p<1x10^{-10}$ for comparison of ICAM-targeted liposome lung uptake vs. IgG liposome lung uptake. ‡:

$p<1x10^{-10}$ for comparison of ICAM-targeted+FI liposome lung uptake vs. IgG+FI liposome lung uptake. Statistical significance was determined via two-way ANOVA with Tukey's correction for multiple comparisons.

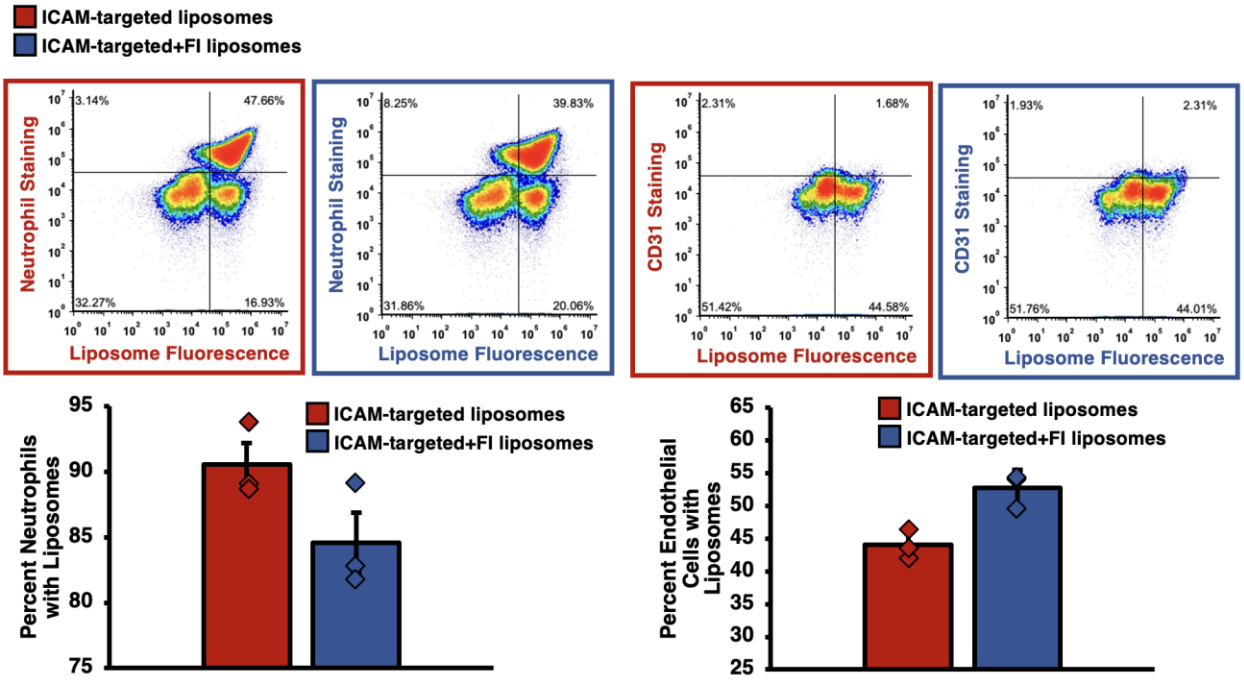

Supplementary Figure 17. Flow cytometry analysis of ICAM-targeted liposome distribution to neutrophils and endothelial cells in the lungs as in figure 3d-e in the main text. Upper panels: Anti-Ly6G neutrophil stain (left) or anti-CD31 endothelial stain vs. liposome fluorescence for single cell suspensions prepared from the lungs of mice receiving ICAM-targeted or ICAM targeted+Factor I liposomes. Lower panels: Percent of neutrophils (left) or endothelial cells (right) positive for liposome fluorescence in mouse lungs treated with ICAM-targeted or ICAM targeted+Factor I liposomes.

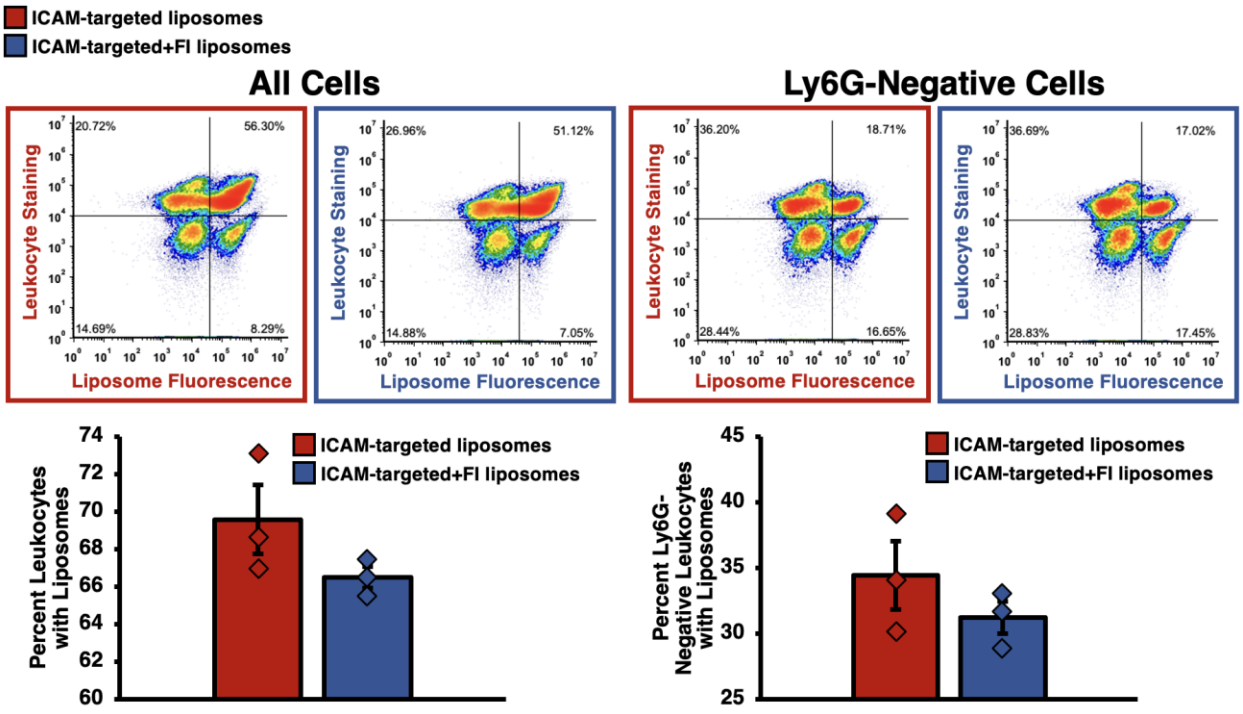

Supplementary Figure 18. Flow cytometry analysis of ICAM-targeted liposome distribution to leukocytes in the lungs as in figure 3d-e in the main text. Upper panels: Anti-Ly6G CD45 leukocyte stain vs. liposome fluorescence for single cell suspensions prepared from the lungs of mice receiving ICAM-targeted or ICAM targeted+Factor I liposomes. Panels to the left indicate analysis of CD45 staining over all cells and panels to the right indicate analysis of CD45 staining over only Ly6G-negative cells (*i.e.*, cells that are not neutrophils). Lower panels: Percent of all leukocytes (left) or leukocytes aside from neutrophils (right) positive for liposome fluorescence in mouse lungs treated with ICAM-targeted or ICAM targeted+Factor I liposomes.

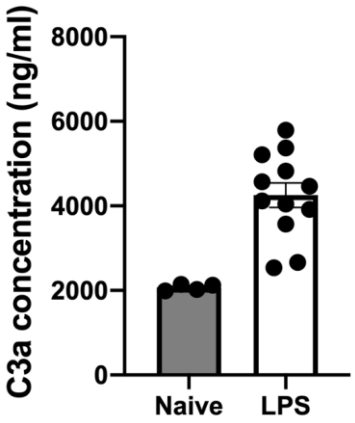

Supplementary Figure 19. ELISA results measuring plasma C3a concentrations in naïve mice and mice treated with intravenous LPS.

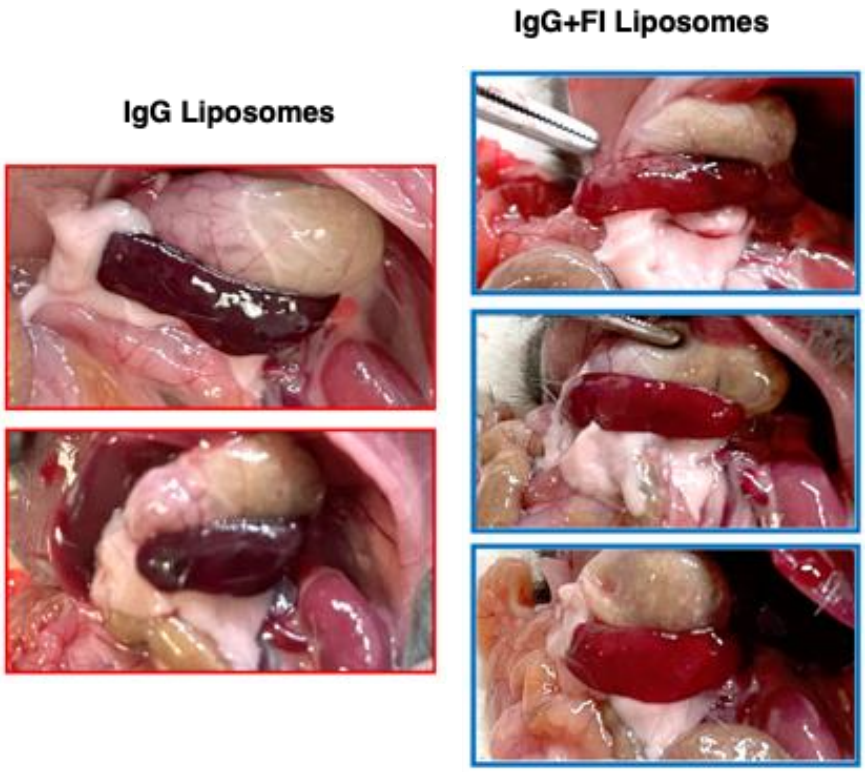

Supplementary Figure 20. Images of spleens of mice treated with IgG liposomes or IgG+factor I liposomes. All mice were treated with IV LPS five hours before liposomes.

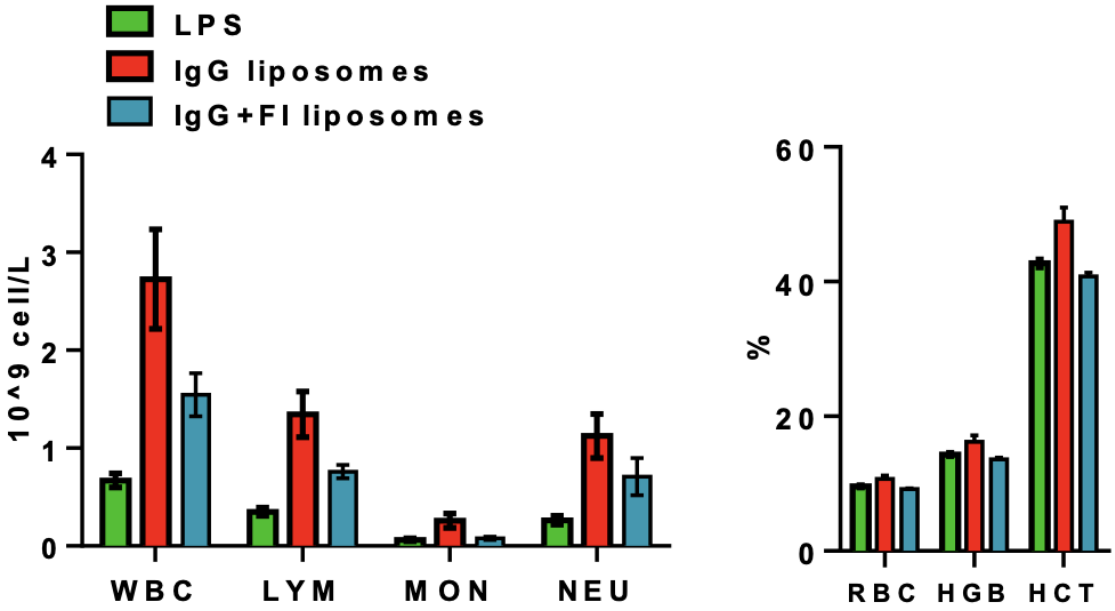

Supplementary Figure 21. Complete blood count data from IV LPS-affected mice receiving IgG liposomes or IgG+Factor I liposomes, expanding on findings presented in figure 4c in the main text.

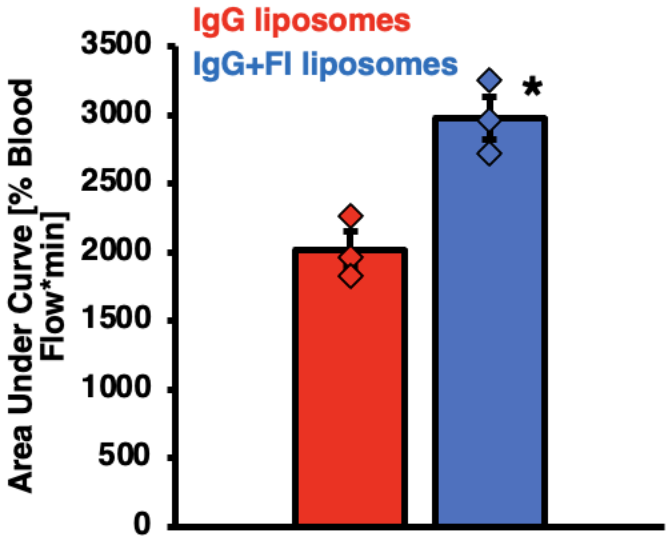

Supplementary Figure 22. Area under curve analysis of middle cerebral artery blood flow in IV LPS-affected mice receiving IgG or IgG+Factor I liposomes.

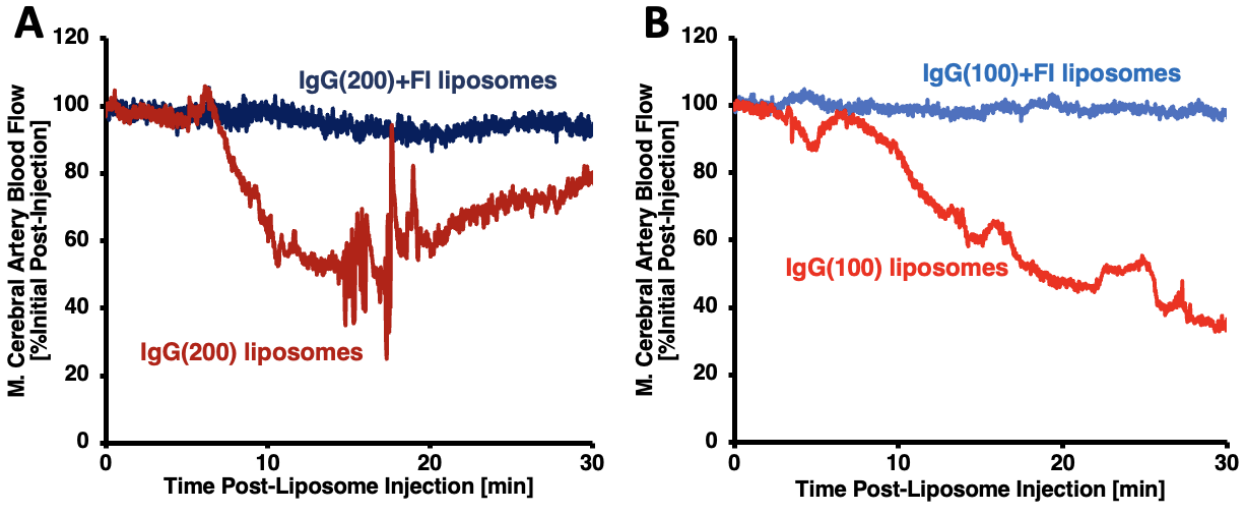

Supplementary Figure 23. Blood flow rate in the middle cerebral artery of IV LPS-affected mice after treatment with IgG or IgG+Factor I liposomes. (a) Data for liposomes with high IgG surface density. (b) Data for liposomes with lower IgG surface density.